MOLECULAR AND CELLULAR BIOLOGY, Oct. 2003, p. 7055–7067 Vol. 23, No. 19
0270-7306/03/$08.00+0 DOI: 10.1128/MCB.23.19.7055–7067.2003

Identification of mRNAs Associated with αCP2-Containing RNP Complexes

Shelly A. Waggoner and Stephen A. Liebhaber*

Departments of Genetics and Medicine, University of Pennsylvania School of Medicine, Philadelphia, Pennsylvania 19104

Received 12 March 2003/Returned for modification 10 June 2003/Accepted 1 July 2003

Posttranscriptional controls in higher eukaryotes are central to cell differentiation and developmental programs. These controls reflect sequence-specific interactions of mRNAs with one or more RNA binding proteins. The α-globin poly(C) binding proteins (αCPs) comprise a highly abundant subset of K homology (KH) domain RNA binding proteins and have a characteristic preference for binding single-stranded C-rich motifs. αCPs have been implicated in translation control and stabilization of multiple cellular and viral mRNAs. To explore the full contribution of αCPs to cell function, we have identified a set of mRNAs that associate in vivo with the major αCP2 isoforms. One hundred sixty mRNA species were consistently identified in three independent analyses of αCP2-RNP complexes immunopurified from a human hematopoietic cell line (K562). These mRNAs could be grouped into subsets encoding cytoskeletal components, transcription factors, proto-oncogenes, and cell signaling factors. Two mRNAs were linked to ceroid lipofuscinosis, indicating a potential role for αCP2 in this infantile neurodegenerative disease. Surprisingly, αCP2 mRNA itself was represented in αCP2-RNP complexes, suggesting autoregulatory control of αCP2 expression. In vitro analyses of representative target mRNAs confirmed direct binding of αCP2 within their 3′ untranslated regions. These data expand the list of mRNAs that associate with αCP2 in vivo and establish a foundation for modeling its role in coordinating pathways of posttranscriptional gene regulation.

Programs of gene expression in eukaryotic cells are coordinated at multiple levels. A significant component of these controls is mediated by posttranscriptional mechanisms. Processing, transport, localization, stability, and translation of an mRNA are often controlled via sequence-specific interactions with RNA binding proteins. Most of these interactions are discovered in the course of exploring specific pathways of gene regulation. Such gene-specific discovery approaches, while highly informative, are not able to focus on the wider impact of particular RNA binding proteins on cell function. A complementary approach that can more effectively address this question would involve the identification of the full spectrum of mRNA targets for a particular RNA binding protein (46). Such an approach would set the stage for constructing an integrated view of how particular RNA binding proteins contribute to coordination of gene expression profiles (21).

Limited examples of coordinate control by RNA binding proteins can be cited from the literature. An initial example is represented by the iron response element binding protein (8). This iron-binding protein can reversibly block translation of ferritin mRNA via 5′ untranslated region (UTR) binding and reversibly stabilize transferrin receptor mRNA via 3′ UTR binding. These distinct actions of the iron response element binding protein coordinate an integrated cellular response to intracellular iron levels. By defining the full-spectrum target mRNAs for specific RNA binding proteins, it may be possible to define even more complex posttranscriptional control networks. Recent examples are the identification of subsets of mRNAs bound by the K homology (KH)-domain fragile X mental retardation protein (5) and segregation of nuclear mRNAs into distinct sets of RNPs during nuclear-cytoplasmic export (17). The concept of coordinate control of multiple genes by RNA-binding proteins has been recently proposed in terms of posttranscriptional operons (21).

The α-globin poly(C) binding proteins (αCPs), also known as hnRNP E (34) or poly(C) binding proteins (PCBP) (1, 23, 24), comprise a family of highly abundant and widely expressed RNA binding proteins. Multiple αCP isoforms are encoded by four dispersed paralogous loci (29, 31, 32, 48). The two most abundant and widely expressed of these proteins, αCP2 and αCP2-KL, are encoded by alternative splicing of the αCP2 transcript (10). αCPs are conserved across several genera: orthologues of αCPs are found in *Xenopus laevis*, *Drosophila melanogaster*, *Caenorhabditis elegans*, and *Saccharomyces cerevisiae* (32). The abundant expression, widespread tissue distribution (24, 29, 31), and evolutionary conservation of αCPs suggest that they serve fundamental functions.

Each αCP isoform contains a characteristic triple repeat of the 70-amino-acid heteronuclear ribonucleoprotein (hnRNP) KH domain. The KH domain is common to a wide spectrum of RNA binding proteins (13) and can interact via a molecular vise with four to five contiguous bases in a target RNA (25, 26). Since KH domains can interact independently with RNA sequences, arrays of such motifs in a protein can generate substantial complexity and specificity of RNA interactions.

αCPs have a characteristic preference for binding to single-stranded C-rich motifs, and binding to these elements has been linked to a number of posttranscriptional controls (2, 12, 35, 36, 38, 45, 52, 53). The initial function defined for αCPs was

* Corresponding author. Mailing address: Department of Genetics, University of Pennsylvania School of Medicine, Room 428, Clinical Research Building, 415 Curie Blvd., Philadelphia, PA 19104. Phone: (215) 898-7834. Fax: (215) 573-5157. E-mail: liebhabe@mail.med.upenn.edu.

TABLE 1. RT-PCR primers

mRNA	DNA length (bp)	Primer set (forward, reverse)[a]
α-Globin	315	5′-GTGGACGACATGCCCAACGC-3′, 5′-CCCACTCAGACTTTATTCAA-3′
γ-Globin	279	5′-AAGGTGCTGACTTCCTTGGG-3′, 5′-ATCCTTGAAAGCTCTGCATC-3′ (49)
GAPDH	180	5′-CAACTACATGGTTTACATGTTC-3′, 5′-GCCAGTGGACTCCACGAC-3′
SAP49	270	5′-AACCGCTGCTGTGGGAACTGTTTC-3′, 5′-GCAACTTCTCATCAATCTCAGGGTC-3′
SAP62	361	5′-CACTTCACAACAATGAGGGGAGC-3′, 5′-AAGGCAATGGTCTCGTAGGGTTCG-3′
Trx2	239	5′-TTGGCTGACAAGCAGGGATGAG-3′, 5′-AAAGGCGTATGGGAGGGAAGAC-3′
αCP2,[b] αCP2-KL	360, 330, 237	5′-GGGGTACCTGTTCTAGCTGCWCCCCAT-3′ (RT), 5′-CGTGACCATYCCGTACC-3′, 5′-TTTGGAATGGTGAGTTCATG-3′ (29)
C-Src	328	5′-GGAACAAAGTCGCCGTCAAGTG-3′, 5′-TCCTCAGACACCAGCACATTGC-3′
JunD	230	5′-GAGAAGAACAGAGTGTTCGAT-3′, 5′-ACAGGAATGTGGACTCGTAGC-3′
A-Raf-1	113	5′-AAAGTATACCTGCCCAACAA-3′, 5′-CAGCAGTCCTGATTTAGACC-3′
Cln2	267	5′-TCCCCACTGCTACTACCTTA-3′, 5′-CAAGAGTGAGAGTTCCTTGG-3′
PPT2	215	5′-CCTCTCCACAGATGGGACAGTATG-3′, 5′-GGCATTGGGATGGTCTCTTTCC-3′
coxll	106	5′-GCAAACCACAGTTTCATGCC-3′, 5′-GGCTCTAGAGGGGGTAGAGG-3′ (49)

[a] In all reactions except for αCP2 amplifications, the reverse primer was used for RT as well as the PCR.
[b] The RT primer is indicated (RT) followed by the forward and reverse primers.

stabilization of human α2-globin (α-globin) mRNA (6, 23, 52, 53) via binding to a 3′ UTR C-rich motif (52). αCP1 and αCP2 have also been linked to stabilization of α1(I) collagen and tyrosine hydroxylase mRNAs via interacting with respective C-rich 3′ UTR motifs (38, 45). Based on these and other studies (9, 55), it has been proposed that the complex between αCP and the *cis*-acting stability elements, referred to as the α-complex (52), constitutes a general determinant of high-level mRNA stability (18).

In addition to its role in mRNA stabilization, αCP also functions in a range of translation controls. Binding of αCP1 and hnRNP K to the 3′ UTR of 15-lipoxygenase mRNA maintains the mRNA in a translationally silent state until the final stages of erythroid differentiation (35). αCP2-mediated translational control also appears to be involved in the pathological block in CCAAT/enhancer binding protein α (c/EBPα) expression in myelogenous leukemia via binding to a C-rich intercistronic motif (39). αCPs can also facilitate translation of cellular mRNAs. For example, translational activation is mediated by binding of αCP to the 5′ UTR of the folate receptor α mRNA (54) and binding to a 3′ UTR C-rich motif in the phosphatase 2A mRNA (36). αCPs bind to several viral mRNAs, and the corresponding RNP complexes are involved in many aspects of the viral life cycle (3, 4, 7, 11, 12, 14, 16, 33, 37, 44, 51). Several of these studies indicate that functional interactions may be specific for particular αCP isoforms, may work in conjunction with additional RNA binding proteins, and may be impacted by cellular differentiation (7, 35).

Five mRNAs have been identified in a screen for αCP1 binding targets: mitochondrial NADH dehydrogenase subunit 3, mitochondrial cytochrome *c* oxidase subunit II (coxII), ribosomal protein of the large subunit (L27a), palmitoylated erythrocyte membrane protein p55, manganese superoxide dismutase, and the CD81 receptor (TAPA-1) (49). The mRNAs encoding TAPA-1 and coxII were further shown to contain αCP1 binding sites in the 3′ UTRs by in vitro binding assays. It is unknown whether these mRNAs constitute αCP1 binding targets in vivo, and the function of these αCP1-RNP complexes remains undefined.

The variety of αCP targets and control mechanisms suggests that the αCP-RNP complexes play significant and multifaceted roles in gene expression. Identification of additional mRNA targets would facilitate further exploration of this potential. In this study, we have attempted to identify a spectrum of in vivo binding targets of the major αCP2 isoforms by microarray analysis of immunopurified cytoplasmic αCP2-RNPs. Three independent studies revealed that 160 mRNAs were specifically and reproducibly present in the αCP2-RNP complexes. These data expand the list of αCP2 binding mRNAs and suggest targets for subsequent studies of potential coordinated cell functions.

MATERIALS AND METHODS

Preparation of cytoplasmic extracts. Extracts were prepared (20) from logarithmically growing (0.5×10^6 to 1.0×10^6 cells/ml) K562 cells (ATCC no. CCL-243) grown under standard conditions. Cells were harvested by centrifugation at $258 \times g$ for 5 min at 4°C, washed with 150 packed cell volumes (pcv) of phosphate-buffered saline (PBS) (Invitrogen) and washed again in 2 pcv of PBS. After sedimentation at $157 \times g$ for 5 min at 4°C, the pellets were resuspended in 3.1 pcv of extraction buffer (15 mM Tris HCl [pH 7.4], 15 mM $MgCl_2$, 150 mM NaCl, and 0.65% Igepal). The lysate was incubated on ice for 10 min with shaking and centrifuged at $11,750 \times g$ for 10 min at 4°C. The cytoplasmic lysate was supplemented with 1 mM phenylmethylsulfonyl fluoride (PMSF) (Sigma), 3 μg of leupeptin/ml (Roche), 1 μg of aprotinin/ml (Sigma), and 13% glycerol and was stored at −80°C.

RNP IP. Protein A-Sepharose (PAS) (Amersham) was washed three times in PBS (Invitrogen) at room temperature. Two hundred microliters of a 50% slurry of PAS and PBS was incubated with 5 μl of FF3 (anti-αCP2 and αCP2-KL) or anti-c-*myc* (Santa Cruz) antibodies in the presence of 0.35 U of anti-RNase/μl (Ambion) in PBS in a volume of 1.0 ml. The FF3 immunoprecipitates (IPs) are referred to as anti-αCP2, and the c-*myc* IPs are referred to as control. The mixtures were incubated for 1 h at 4°C, and the PAS was washed once with PBS. The K562 cytoplasmic extract (2.1 mg/IP) was centrifuged at $11,750 \times g$ for 10 min at 4°C. The supernatant was diluted fourfold in binding buffer (BB) (20 mM HEPES [pH 7.9] and 150 mM NaCl) containing 0.05% Triton X-100. Anti-RNase (Ambion) was added to 0.15 U/μl. This extract was added to the PAS, incubated for 1 h at 4°C, and washed twice in BB containing 0.05% Triton X-100, followed by two washes in BB containing 1% Triton X-100. The PAS was resuspended in BB containing 0.05% Triton X-100, and the suspension was transferred to a fresh tube. The PAS was pelleted and resuspended in elution buffer (100 mM Tris-HCl [pH 7.4], 12.5 mM EDTA, 150 mM NaCl, and 1% sodium dodecyl sulfate [SDS]). The mixture was incubated for 3 min at 100°C, phenol extracted, ethanol precipitated with glycogen (20 μg; Boehringer), and resuspended in 20 μl of H_2O.

Reverse transcription-PCR. Copurified RNA (1.5 μl) was incubated with 1 pmol of reverse primer (listed in Table 1), 1 mM each dNTPs, 2.5 U of anti-RNase (Ambion), 50 U of Moloney murine leukemia virus reverse transcriptase (Promega), and 1× Moloney murine leukemia virus reverse transcription (RT) buffer (Promega) in a volume of 12.5 μl. After incubation at 37°C for 1 h, the samples were used as a template for PCR. The PCR primers are listed in Table

1. The forward primer (8 pmol) was end labeled by incubation with 5 μl of [γ-^{32}P]rATP (6,000 Ci/mmol), 1× forward reaction buffer (Gibco), and 10 U of T4 polynucleotide kinase (Gibco) for 30 min at 37°C and at 65°C for 10 min. The PCRs included 5 μl of the RT product, 0.2 mM dNTPs, 1.5 mM $MgCl_2$, 2.5 μl of the labeled primer, 2.5 μg of each primer, 0.25 U of AmpliTaq (Perkin Elmer), and 1× PCR buffer II (Perkin Elmer). Thermocycler conditions were 95°C for 3 min followed by 30 cycles of 95°C for 1 min, 52°C for 1 min, and 72°C for 1 min followed by a final cycle of 72°C for 10 min. Samples were visualized by 5% polyacrylamide gel electrophoresis (PAGE) and quantified by the PhosphorImager (ImageQuant; Molecular Dynamics).

Amplification of antisense mRNA probes. The copurified RNA was amplified as described previously (40) with modifications. One hundred picomoles of T7-oligo$(dT)_{24}$ primer (Affymetrix sequence; GenSet Oligos) was added to the RNA. After heating at 70°C for 10 min and 42°C for 5 min, first-strand cDNA was synthesized using the SuperScript Choice kit (InVitrogen). Conditions consisted of 0.01 M dithiothreitol (DTT), 0.5 mM dNTPs, 10 U of Superscript II reverse transcriptase/μl and 1× first-strand buffer in a volume of 20 μl. After incubation at 42°C for 1 h, second-strand cDNA was synthesized with 0.2 mM dNTPs, 0.26 U of DNA polymerase I/μl, 0.013 U of RNaseH/μl, 0.07 U of DNA ligase/μl, and 1× second-strand buffer. The samples were incubated at 16°C for 2 h. T4 DNA polymerase was added (0.07 U/μl) and incubated for 10 min at 16°C. The product was phenol extracted followed by purification using a YM-50 filter (Millipore). Antisense mRNA was synthesized using the T7 MEGAscript kit (Ambion) and was extracted and purified on a YM-50 filter (Millipore). Random hexamers (2 μg; Amersham) were added, and the volume was adjusted to 20 μl. After incubation at 70°C for 10 min, on ice for 2 min, and at room temperature for 10 min, first-strand cDNA was synthesized using the SuperScript Choice kit (InVitrogen) in a volume of 40 μl. The samples were treated with 0.1 U of RNase H/μl, incubated at 37°C for 20 min and 94°C for 2 min, and placed on ice. T7-oligo$(dT)_{24}$ primer was added (final concentration, 200 pmol) and incubated at 70°C for 5 min and then at 42°C for 10 min. Second-strand synthesis was performed as described above except that the volume was 300 μl and the DNA ligase was omitted. After incubation at 16°C for 2 h, the product was extracted and purified using a YM-50 filter (Millipore). This double-stranded (ds) cDNA was used in another RNA amplification by repeating the antisense mRNA and ds cDNA synthesis [i.e., with the first strand being primed by using random hexamers and second strand being primed by using the T7-oligo$(dT)_{24}$]. The ds cDNA contained a T7 promoter followed by cDNA encoding the antisense mRNA of the copurified mRNA. This cDNA was then used as template to generate radiolabeled antisense mRNA to probe the slot blot or to generate biotinylated antisense mRNA to probe the microarray (see below).

In vitro RNA synthesis. ^{32}P-labeled RNA for the slot blot hybridization was synthesized using the T7 MEGAshortscript kit (Ambion). The ds cDNA from the antisense mRNA amplification (see above) was used as a template. The final concentration of rATP, rGTP, and rUTP was 5.6 mM, and the final concentration of unlabeled rCTP was 0.08 mM. Three microliters of [α-^{32}P]rCTP (400 Ci/mmol) was used per reaction. The RNA was purified using an RNAeasy column (Qiagen), and 3.3×10^6 cpm of probe was used per slot blot.

Biotinylated RNA probe for the microarray hybridization was synthesized using a BioArray high-yield RNA transcript labeling kit (Enzo). The ds cDNA from the antisense mRNA amplification (see above) was used as a template. The RNA was purified, quantified, and fragmented according to Affymetrix protocols. Equal masses of probe (7 to 12 μg/microarray for three studies) were used for each set of microarrays.

4-thio-rUTP RNA probes for the cross-linking studies were synthesized as described previously (50). Two micrograms of *Eco*RI-linearized pSP6-(Trx2 or SAP49 or α-Globin)3′UTRpolyA (see below) and 1 μg of pTRI-β-actin-mouse (which generates β-actin antisense RNA) (Ambion) were used as template. The Maxiscript SP6 kit (Ambion) was utilized with final concentrations of rUTP (0.5 mM), rCTP (12 μM), and 4-thio-rUTP (0.25 mM) and 2.6 μl of [α-^{32}P]rCTP (3,000 Ci/mmol). The RNA was purified using an RNAeasy column (Qiagen), and 1.5×10^6 cpm of RNA was used per reaction.

RNA probes for the electrophoretic mobility shift assay (EMSA) studies were generated using the Maxiscript SP6 kit (Ambion) with 1 μg of *Eco*RI-linearized pSP6-(Trx2 or SAP49 or α-Globin)3′UTRpolyA, 0.5 μg of pTRI-β-actin-mouse (Ambion), with a rCTP (12 μM) and 5 μl of [α-^{32}P]rCTP (400 Ci/mmol). RNA was purified (RNAeasy; Qiagen), and 7×10^5 to 9×10^5 cpm of RNA was used in each EMSA.

Slot blot hybridization. Tenfold dilutions of plasmids (8 to 800 ng) containing the cDNAs encoding hα2-globin and β-actin cDNA or PUC19 vector were diluted 100-fold in 0.4 M NaOH, transferred via slot blot vacuum manifold to Zetabind nylon (Cuno), and incubated in 0.4 M NaOH at room temperature for 5 min. The membrane was neutralized in 0.2× SSC (1× SSC is 150 mM NaCl and 15 mM sodium citrate)–0.2 M Tris (pH 7.5) at room temperature for 2 min and cross-linked in the UV Stratalinker 2400 (autocross-link) (Stratagene). The membrane was washed in 0.1× SSC–0.1% SDS at 65°C for 30 min and prehybridized in 0.5 M $NaPO_4$ (pH 7.2), 7% SDS, 1% bovine serum albumin, and 0.1 mM EDTA at 65°C for 4 h. Then, 3.3×10^6 cpm was incubated with the membrane at 42°C overnight in a buffer of 5× SSC, 5× Denhardt's, 50% formamide and 1% SDS. After washing two times with 1× SSC–0.1% SDS at 42°C for 15 min and at 42°C for 30 min, the membranes were rinsed in 2× SSC and exposed to the PhosphorImager, and signals were quantified (ImageQuant; Molecular Dynamics).

Microarray hybridization and data analysis. The biotinylated cRNAs were hybridized to the Affymetrix human genome U95A microarrays at the MIT biopolymers lab. For each set of microarray experiments, an equal mass of antisense RNA was used as the probe. The image ("dat") files were analyzed using Microarray Suite (MAS) version 5.0 (Affymetrix). A comparison analysis was performed between the experimental αCP2 microarray and the baseline control microarray for each experiment. The comparison files for each of three independent experiments were compiled into a single Excel file. This file was sorted to include those mRNAs that were designated "present" (i.e., detected) by MAS and those which showed an enrichment in the αCP2 microarray relative to the control microarray. The cutoff value for enrichment was twofold. The signal log ratio value, which reflects the abundance of an mRNA, was averaged among the three independent microarray experiments for each mRNA. This average signal log ratio was used to calculate the fold enrichment according to equations from Affymetrix. These fold enrichment values were normalized to the fold enrichment value calculated for the γ-globin mRNA negative control. The individual normalized fold change (INFC) for each independent microarray experiment and the averaged normalized fold change (Avg NFC) for all three studies are represented in Table 2. The ranking of the mRNAs is based on the Avg NFC value.

Cloning of the Trx2 and SAP49 3′ UTRs. The 3′ UTRs of Trx2 and SAP49 were amplified using primers that contained *Hind*III or *Sac*I sites (underlined), namely, 5′AAGCTTGCTGATTGGCTGACAAGCAGGG3′ and 5′GAGCTC GACATTGCAGATGGTGCAGACCC3′ (for Trx2) and 5′AAGCTTCAGTAA ATTCACATTTTCCTTCC3′ and 5′GAGCTCAAACAAGGAGTTTAGTTTT ATTTTC3′ (for SAP49). The templates for PCR were human I.M.A.G.E. clones 2446364 (Trx2) and 38675 (SAP49) from Research Genetics. The PCRs consisted of the following: 0.2 mM dNTPs, 1.5 mM $MgCl_2$, 0.05 μg of each primer, 1× PCR Buffer II (Roche), 0.04 μg of template, and 1.25 U of AmpliTaq (Roche). The conditions were 95°C for 3 min; 20 cycles of 94°C for 1 min, 56°C (SAP 49) or 64°C (Trx2) for 1 min, and 72°C for 1 min; and 72°C for 10 min. Fragments were gel isolated using Qiaex II (Qiagen) and ligated into pGemT (Promega), and clones were verified by sequencing. Plasmids were digested with *Hind*III and *Sac*I, and the fragments were purified and ligated into the same sites in pSP64polyA (Promega). The constructs contained an SP6 promoter linked to the cDNAs encoding Trx2 or SAP49 3′ UTRs and a (dT-dA)$_{30}$ cassette followed by an *Eco*RI site. These plasmids are named pSP6-(Trx2 or SAP49)3′UTRpolyA. The pSP6-α-Globin 3′UTRpolyA has the same structure described above, except that it contains the 3′UTR of α2-globin mRNA.

RNA binding studies. RNA EMSAs were carried out as described previously (6). UV cross-linking reactions were performed as described previously (50) with modifications. Thirty-five micrograms of the K562 extract was incubated in cross-linking buffer (8.5 mM HEPES [pH 7.4], 3.0 mM $MgCl_2$, 27.0 mM KCl, and 1.0 mM DTT) with RNA (6×10^6 cpm; 90 nM) in the presence or absence of unlabeled competitor RNA. After irradiation and RNase digestion, the samples were immunoprecipitated with FF3 or control antibodies using the conditions described above for the RNP IP. The products were resolved by SDS–10% PAGE. Competition experiments were analyzed by the PhosphorImager and quantitated using ImageQuant (Molecular Dynamics).

RESULTS

Verification of αCP-RNP IP: α-Globin mRNA interacts with αCP in vivo. An αCP2-RNP IP strategy was established to isolate and identify a set of mRNAs that interact in vivo with αCP2 and its major splice variant form, αCP2-KL. The K562 cell line was chosen for this analysis. This human erythroid cell line contains high levels of human α-globin and γ-globin mRNAs which can serve as positive and negative controls, respectively, for the IP reaction; interaction of α-globin mRNA

TABLE 2. mRNAs (160) enriched in the αCP2 immunoprecipitate relative to the control immunoprecipitate

mRNA type and name	Probeset I.D.[a]	Accession no.[b]	Avg NFC[c] (INFC[d])	Rank[e]
Splicing factors				
Spliceosomal protein (SAP62)	37462_i_at	L21990	80 (57, 73, 96)	1
U1 snRNP-specific protein A	40842_at	M60784	22 (12, 15, 45)	14
Spliceosomal protein (SAP49)	33909_at	L35013	20 (9, 16, 42)	20
Splicing factor (SF3a120)	34733_at	X85237	8 (4, 6, 17)	117
Enzymes				
Glutathione *S*-transferase subunit 4	39054_at	X08020	71 (27, 90, 118)	2
Pancreatic kallikrein	246_at	M25629	29 (22, 28, 31)	7
Ubiquitin-conjugating enzyme 5B (UBCH5B)	832_at	U39317	21 (12, 18, 32)	18
Na^+, K^+ ATPase beta 2 subunit	37270_at	AF007876	18 (10, 14, 34)	25
Glutathione *S*-transferase M4	556_s_at	M96233	15 (9, 16, 21)	37
NADH-cytochrome B5 reductase	36668_at	M28713	15 (6, 19, 24)	39
Lysosomal pepstatin-insensitive protease (CLN2)	32824_at	AF039704	13 (7, 11, 24)	54
FK506-binding protein	880_at	M34539	13 (8, 12, 17)	59
Vacuolar H^+ ATPase proton channel subunit	36994_at	M62762	12 (9, 10, 16)	63
Lysophosphatidic acid acyltransferase alpha	32836_at	U56417	12 (6, 12, 20)	68
Palmitoyl-protein thioesterase 2 (PPT2)	38108_at	AF020543	10 (4, 8, 20)	103
Pyruvate kinase L	37077_at	D13243	9 (4, 7, 21)	107
Calcium ATPase (HK1)	39791_at	M23114	7 (3, 6, 15)	139
5-Aminolevulinate synthase (ALAS)	37285_at	X60364	6 (3, 6, 9)	154
Cytoskeleton structure or motility				
Rho GDP-dissociation inhibitor 1	40164_at	X69550	47 (26, 55, 57)	4
Profilin	36675_r_at	J03191	42 (15, 42, 90)	6
Dynamin	32138_at	L07807	24 (14, 15, 55)	9
F-Actin capping protein beta subunit	37012_at	U03271	18 (6, 21, 34)	27
EB3	40825_at	AB025186	17 (12, 18, 20)	28
Human serum constituent protein (MSE55)	38132_at	M88338	15 (6, 19, 22)	40
Suppressor of yeast actin mutation 2 homologue	32658_at	AL031228	13 (8, 12, 16)	58
Mutant β-actin (ACTB)	32318_s_at	X63432	12 (4, 19, 20)	67
MacMarcks	36174_at	X70326	11 (6, 11, 20)	74
BA46 (lactadherin)	34403_at	U58516	11 (3, 10, 30)	82
Leukosialin (sialophorin)	36798_g_at	J04168	10 (7, 8, 13)	101
Dematin 52-kDa subunit	37192_at	U28389	9 (7, 8, 10)	111
Phospholipase D	934_at	L11702	8 (5, 5, 17)	128
BAI-associated protein 2 alpha (BAP2-alpha)	37760_at	AB015019	7 (4, 8, 10)	134
Mitochondrial enzymes				
Uncoupling protein homologue (UCPH)	37591_at	U94592	27 (17, 25, 39)	8
Mitochondrial thioredoxin (Trx2)	32852_at	U78678	13 (9, 10, 16)	60
Mitochondrial nucleoside-diphosphate kinase	39089_at	Y07604	11 (6, 10, 18)	78
Outer membrane mitochondrial translocase	37049_g_at	U58970	10 (5, 11, 12)	97
Citrate synthase	41314_at	AF047042	7 (4, 5, 12)	145
NAD(H)-specific isocitrate dehydrogenase	36574_at	Z68907	6 (4, 5, 8)	151
Transcription factors				
Mel-18	32192_g_at	D13969	24 (10, 30, 36)	11
T-cell factor 1, splice form C	32649_at	X59871	21 (7, 17, 63)	16
Pleomorphic adenoma gene-like 1 (PLAGL1)	36943_r_at	U81992	17 (11, 12, 26)	30
Homeodomain protein DLX-2	34585_at	L07919	15 (11, 14, 18)	35
Homeodomain protein HOXC6	40674_s_at	S82986	14 (9, 13, 21)	46
ROX protein	35145_at	X96401	12 (7, 14, 16)	61
Upstream stimulatory factor 2 (USF2)	39112_at	Y07661	12 (10, 10, 15)	66
High-mobility group protein (HMG-I(Y))	39704_s_at	L17131	12 (5, 15, 16)	73
JunD	41483_s_at	X56681	8 (5, 5, 17)	119
NF-κB p65 subunit	1295_at	L19067	8 (3, 9, 15)	120
NF-κB p65 subunit	36645_at	L19067	8 (4, 10, 10)	125
Apolipoprotein AI regulatory protein (ARP-1)	39397_at	M64497	8 (4, 6, 14)	127
RNA polymerase II largest subunit	40791_at	X63564	7 (4, 5, 14)	135
T-cluster binding protein	41763_g_at	D64015	7 (4, 6, 11)	140
G protein pathway suppressor 2 (GPS2)	35653_at	U28963	6 (4, 6, 7)	149
Protein kinases				
c-*src* kinase	1768_s_at	X59932	11 (7, 8, 18)	77
Casein kinase II (CKII) β-subunit	410_s_at	X57152	10 (5, 12, 13)	87
A-Raf-1 kinase	1706_at	U01337	10 (8, 9, 11)	90

Continued on following page

TABLE 2—*Continued*

mRNA type and name	Probeset I.D.[a]	Accession no.[b]	Avg NFC[c] (INFC[d])	Rank[e]
Myt1 kinase	480_at	U56816	10 (6, 8, 15)	95
MAP kinase kinase 5 (MEK5)	513_at	U25265	10 (4, 10, 20)	100
Extracellular signal-regulated kinase 1 (ERK1)	1000_at	X60188	9 (5, 10, 13)	106
Cell growth and proliferation				
KIP2	39903_at	AB012955	45 (22, 29, 110)	5
Insulin-like growth factor binding protein 4	39781_at	U20982	16 (11, 14, 22)	32
Thromboxane A2 receptor	336_at	D38081	13 (9, 12, 16)	55
Insulin-like growth factor binding protein 4	1737_s_at	M62403	13 (6, 13, 20)	57
Neurite outgrowth-promoting protein	38124_at	X55110	11 (5, 9, 26)	75
Calpain small subunit 1 (CAPNS1)	36138_at	X04106	11 (8, 9, 13)	84
Epidermal growth factor response factor 1	38740_at	X79067	10 (5, 7, 26)	85
Midkine (MK)	577_at	M94250	10 (4, 12, 17)	89
14-3-3σ (stratifin)	33323_r_at	X57348	10 (4, 11, 17)	92
14-3-3ε	1011_s_at	U54778	10 (5, 7, 22)	96
Phosphotyrosyl phosphatase 2A activator	39127_f_at	X73478	10 (5, 11, 12)	104
Protein phosphatase 6 (PP6C)	37581_at	X92972	8 (5, 5, 14)	123
Cyclin I	1836_at	D50310	7 (5, 6, 8)	142
Connector enhancer of KSR-like protein (CNK1)	38221_at	AF100153	5 (2, 4, 11)	159
Interferon-inducible factors				
Interferon-inducible gene I-8D	411_i_at	X57351	22 (6, 33, 39)	15
Interferon-induced transmembrane protein 3	41745_at	X57352	10 (5, 13, 13)	88
Interferon-inducible protein 9-27	676_g_at	J04164	8 (7, 7, 9)	118
Polymeric immunoglobulin receptor	34005_at	X73079	6 (4, 4, 10)	156
RNA binding proteins				
αCP-2	35746_r_at	X78136	12 (6, 12, 20)	69
αCP-2	35745_f_at	X78136	11 (6, 9, 17)	83
E1B 55 kDa-associated protein	40106_at	AJ007509	9 (8, 8, 10)	108
Staufen	41823_at	AJ132258	6 (4, 5, 9)	152
Poly(A) binding protein	31950_at	Y00345	5 (2, 6, 7)	160
Other				
Alpha subunit of hemoglobin	31525_s_at	J00153	53 (34, 48, 70)	3
Vacuolar ATPase 14-kDa subunit	37395_at	D49400	22 (15, 21, 28)	13
Clone RP1-37E16 on chromosome 22	34046_at	z83844	20 (11, 13, 48)	19
Negative 14 gene	40956_at	X90857	19 (10, 18, 28)	23
XE169	33268_at	L25270	18 (10, 12, 42)	24
Cosmid ICK0721Q.4.1 (PHD finger protein 2)	40446_at	AL021366	15 (7, 20, 20)	41
Solute carrier family 7, member 8 (SLC7A8)	41271_at	Y18483	15 (8, 15, 22)	42
Cleft lip and palate transmembrane protein	41413_at	AF037339	15 (11, 14, 16)	44
Lymphocyte-secreted C-type lectin precursor	37147_at	AF020044	14 (7, 12, 28)	48
TPRC gene	39149_at	X99720	14 (11, 12, 16)	49
28-kDa heat shock protein (hsp28)	36785_at	Z23090	12 (6, 12, 20)	62
Amine oxidase pseudogene	31626_i_at	AF047485	10 (4, 10, 24)	86
OXA1Hs	39774_at	X80695	10 (5, 10, 17)	93
Homologue of yeast Rad23 protein A (hHR23A)	41197_at	D21235	10 (6, 9, 14)	94
HSU93305	37326_at	U93305	10 (6, 10, 12)	99
OS-9	36996_at	U41635	10 (7, 10, 10)	102
Ras-related protein Rab5b	37362_at	X54871	9 (6, 6, 17)	112
Clone C3 CHL 1 protein (CHLR1)	31935_s_at	U75968	9 (4, 8, 14)	114
Major histocompatibility complex class I molecule	35937_at	U65416	9 (4, 7, 20)	115
Na^+/H^+ exchanger 1 (NHE-1)	32681_at	S68616	8 (4, 7, 13)	124
Clone 886K2 on chromosome 1p35.1-36.12	36986_at	AL031295	7 (4, 6, 14)	133
G protein coupled receptor (GPR19)	156_s_at	U64871	7 (2, 7, 15)	141
G (i) protein alpha subunit	37307_at	X04828	6 (4, 5, 10)	147
HLA-DMB	41609_at	U15085	6 (4, 5, 10)	148
C1D protein	39782_at	X95592	6 (2, 8, 10)	155
Unknown function				
17b9 *Homo sapiens* cDNA	32389_at	W25892	24 (18, 23, 28)	10
mRNA for hypothetical protein	38483_at	AJ011916	24 (14, 21, 36)	12
ow26f02.x1 *H. sapiens* cDNA	38663_at	AI033692	21 (14, 16, 32)	17
Ataxin-2 related protein	34817_s_at	U70671	19 (9, 17, 36)	21
Homologue of yeast KDEL receptor	37387_r_at	X55885	19 (9, 14, 42)	22
43h8 *H. sapiens* cDNA	39773_at	W28235	18 (15, 16, 20)	26

Continued on following page

TABLE 2—*Continued*

mRNA type and name	Probeset I.D.[a]	Accession no.[b]	Avg NFC[c] (INFC[d])	Rank[e]
KIAA0048 gene	37212_at	D28588	17 (9, 12, 36)	29
zh49e04.s1 *H. sapiens* cDNA	38726_at	W80399	16 (12, 14, 20)	31
KIAA1100 gene	41179_at	AB029023	16 (8, 11, 36)	33
wl90e10.x1 *H. sapiens* cDNA	41047_at	AI885170	16 (12, 14, 19)	34
wf20e04.x1 *H. sapiens* cDNA	40997_at	AI660963	15 (8, 11, 34)	36
DKFZp566K192_s1 *H. sapiens* cDNA	32243_g_at	AL038340	15 (5, 19, 28)	38
KIAA0269 gene	37190_at	D87459	15 (10, 11, 26)	43
af28f05.s1 *H. sapiens* cDNA	38828_s_at	AA628946	14 (10, 12, 20)	45
zq95f07.s1 *H. sapiens* cDNA	32163_f_at	AA216639	14 (12, 13, 14)	47
yx99b12.r1 *H. sapiens* cDNA	38725_s_at	N36295	14 (10, 13, 16)	50
Glycophorin HeP2	41026_f_at	U05255	14 (8, 9, 26)	51
Myelodysplasia/myeloid leukemia factor 2	37719_at	AF070539	13 (7, 14, 20)	52
KIAA0909 protein	41421_at	AB020716	13 (6, 18, 18)	53
KIAA0253 gene	34835_at	D87442	13 (6, 14, 19)	56
Homologue of yeast KDEL receptor	37386_i_at	X55885	12 (7, 9, 21)	64
Human clone 23722 mRNA sequence	38093_at	U90909	12 (6, 10, 22)	65
Not 56-like protein	38161_at	Y09022	12 (8, 12, 13)	70
Ki nuclear autoantigen	39796_at	U11292	12 (6, 14, 15)	71
AF1q	36941_at	U16954	12 (4, 14, 24)	72
DKFZp586H2219 *H. sapiens* cDNA	39686_g_at	AL050282	11 (7, 7, 24)	76
hPMS3	31600_s_at	D38435	11 (8, 11, 12)	79
Putatively prenylated protein (CXX1)	33856_at	Y13374	11 (7, 11, 14)	80
qy39a10.x1 *H. sapiens* cDNA	39689_at	AI362017	11 (5, 6, 39)	81
Homologue of yeast NOT4 (NOT4H)	32820_at	U71267	10 (7, 9, 12)	91
DKFZp564E242 *H. sapiens* cDNA	38710_at	AL096714	10 (5, 11, 12)	98
mRNA expressed in placenta	35308_at	D83200	10 (5, 10, 13)	105
zd37g06.r1 *H. sapiens* cDNA	32736_at	W68830	9 (4, 7, 20)	109
yx76e06.s1 *H. sapiens* cDNA	34329_at	N25547	9 (6, 9, 10)	110
KIAA0109 gene	39795_at	D63475	9 (7, 8, 10)	113
qo77c11.x1 *H. sapiens* cDNA	38705_at	AI310002	8 (5, 5, 18)	116
qb81g08.x1 *H. sapiens* cDNA	37050_r_at	AI130910	8 (3, 10, 12)	121
KIAA0715 protein	37415_at	AB018258	8 (3, 5, 24)	122
Leucine zipper protein	39158_at	AB021663	8 (4, 6, 14)	126
af28f05.s1 *H. sapiens* cDNA	38829_r_at	AA628946	8 (5, 7, 9)	129
zw93f01.r1 *H. sapiens* cDNA	35805_at	AA447263	8 (5, 8, 8)	130
KIAA0544 protein	32235_at	AB011116	7 (4, 8, 9)	131
DinG	33484_at	Y10571	7 (4, 8, 10)	132
wh92e05.x1 *H. sapiens* cDNA	32540_at	AI762547	7 (4, 5, 16)	136
KIAA1002 protein	41366_at	AB023219	7 (5, 5, 11)	137
tu06g05.x1 *H. sapiens* cDNA	39010_at	AI658639	7 (3, 7, 11)	138
Clone 24487	31961_r_at	AF070579	7 (3, 4, 17)	143
Clone 23704	35304_at	AF052130	7 (4, 5, 14)	144
KIAA0468 protein	32092_at	AB007937	6 (4, 6, 8)	146
Synovial sarcoma (SS) X4 (SSX4)	35950_at	U90841	6 (4, 5, 9)	150
KIAA0058 gene	36616_at	D31767	6 (3, 6, 8)	153
Clone 24723	35328_at	AF055023	6 (3, 3, 16)	157
Clone 24448	34864_at	AF070638	5 (2, 6, 8)	158

[a] Affymetrix probeset identification number.
[b] Genbank accession number.
[c] Avg NFC using γ-globin as the normalization factor. This value reflects the relative enrichment of the mRNA species in the αCP2 immunoprecipitate relative to the control immunoprecipitate.
[d] INFC for each independent microarray hybridization. Note that the average of these three values does not necessarily equal the Avg NFC because the normalization value used for the Avg NFC was an average of the normalization factor (γ-globin) from the three microarray hybridizations.
[e] These rankings are based on the Avg NFC values.

with αCP2 has been previously characterized in detail and has a defined biologic function (23), while γ-globin mRNA lacks αCP binding sites (49). Native αCP2-RNP complexes were immunoprecipitated from K562 cytoplasmic extracts using an affinity-purified rabbit antiserum specific to the two predominant human αCP isoforms, αCP2 and αCP2-KL (anti-αCP2) (6). As a specificity control, a parallel set of IPs (control IP) was carried out using an unrelated rabbit antiserum. Rabbit anti-human c-*myc* was used for this purpose. Parameters were established to maximize the yield and the specificity of αCP2-RNP complex IP (see Materials and Methods). To assess this approach, the relative contents of α-globin or γ-globin mRNAs were compared in the RNA isolated from the anti-αCP2 IP and the control IP by targeted RT-PCR (Fig. 1A). α-Globin mRNA was enriched by 100-fold in the αCP2-RNP IP (lane 1) compared to the control IP (lane 2). In contrast, the contents of γ-globin mRNA in the two preparations were within twofold of each other (lane 3 versus lane 4). As γ-globin mRNA does not interact with αCP, this ratio of γ-globin in the two preparations establishes the background ratio for comparisons of enrichment in each study (see below). These data demonstrate robust enrichment of α-globin mRNA in the αCP2-RNP com-

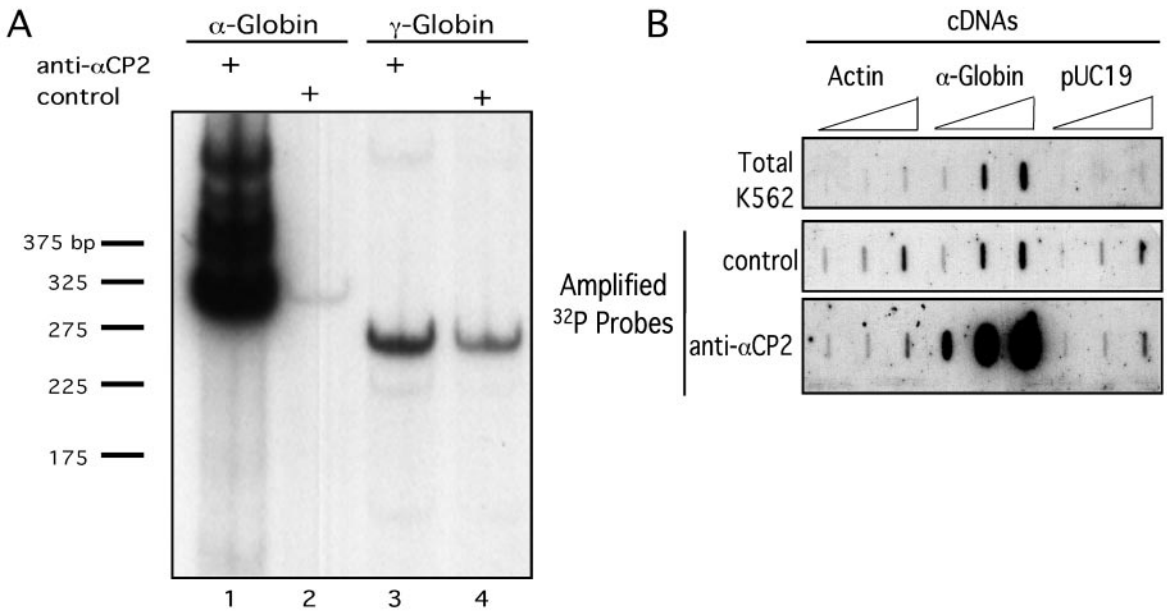

FIG. 1. Isolation of αCP2-RNP complexes. (A) α-Globin mRNA copurifies with αCP2-RNPs isolated from human erythroid (K562) cells. Targeted RT-PCR was carried out on RNA isolated from RNP complexes immunoprecipitated with antiserum specific to the major αCP2 isoforms, αCP2 and αCP2KL (anti-αCP2) (lanes 1 and 3). Analysis of mRNAs isolated from a control IP reaction was carried out in parallel (control) (lanes 2 and 4). Lanes 1 and 2 are targeted amplifications of α-globin mRNA, while lanes 3 and 4 are amplifications of γ-globin mRNA. The autoradiograph was intentionally overexposed to reveal trace levels of α-globin mRNA present in the control lane (lane 2). The numbers on the left represent marker DNA fragments in base pairs. (B) Enriched representation of α-globin mRNA in immunoprecipitated αCP2-RNPs is maintained during probe amplification. cDNAs encoding actin, α-globin, or pUC19 vector sequences were applied to a nylon membrane (8, 80, and 800 ng/slot; see Materials and Methods). The membranes were hybridized with ^{32}P antisense probes generated from unamplified total cellular RNA (Total K562) and from amplified mRNA isolated from control or anti-αCP2 IP reactions.

plexes and establish in vivo association of α-globin mRNA with αCP2 in K562 cells.

α-Globin mRNA enrichment in the αCP2-RNP preparation is maintained during antisense probe amplification. The optimized IP approach was applied to the identification of mRNAs present in αCP2-RNP complexes in K562 cells. To generate sufficient probe for a full set of microarray hybridizations, mRNAs copurified from each RNP preparation were cycled through an amplification protocol (see Materials and Methods). This protocol generates ds cDNAs that carry a T7 promoter. Subsequent in vitro transcription from this T7 promoter generates antisense probes complementary to the initial mRNA pools. To determine whether the representation of mRNAs in the αCP2-RNP complexes is maintained during the amplification procedure, radiolabeled antisense mRNA pools (see Materials and Methods) were used to probe a slot blot containing cDNAs encoding a set of control sequences: α-globin, β-actin, or pUC19. β-Actin represents an mRNA unassociated with αCP2, and pUC19 serves as a control for nonspecific hybridization. The results are shown in Fig. 1B. There was equivalent low-level hybridization to pUC19 sequences and to the β-actin cDNA using probes derived from the anti-αCP2 and control IPs. In contrast, α-globin mRNA was enriched approximately 200-fold relative to the control IP and 55-fold relative to the unfractionated (total) K562 RNA pool. These data demonstrate that the amplification procedure maintains the enrichment of α-globin mRNA and support the validity of carrying out amplification of the RNAs prior to probe generation and microarray hybridization.

Microarray analysis of mRNA content in αCP2-RNPs isolated from K562 cells. Amplified ds cDNAs from the IP reactions were used as templates to generate biotinylated antisense probes for interrogation of Affymetrix human genome U95A microarrays (12,600 open reading frames). A comparison analysis using Microarray Suite software, version 5.0, was performed for each experiment; the αCP2 IP microarray hybridization was designated the experimental microarray, and the control IP microarray hybridization was designated the baseline microarray (see Materials and Methods). Three independent studies were carried out, beginning each time with fresh extract and IP and proceeding through microarray hybridizations (Fig. 2). The total number of mRNAs detected on the microarrays varied by 1.6- to 2-fold among the three independent hybridizations, as did the number of mRNAs that were scored as enriched in αCP2-RNP complexes. Comparison among the data sets revealed a cohort of 160 mRNAs that copurified (i.e., were twofold or more enriched) with αCP2-RNP complexes in all three experiments. These mRNAs were considered a maximally reliable set of in vivo αCP2-binding targets.

Identification and classification of the 160 mRNAs enriched in αCP2-RNPs. The 160 mRNAs that copurified with αCP2 in all three IP studies are displayed in Table 2. Each mRNA is identified by its Affymetrix identification number (Probeset I.D.), GenBank accession number, Avg NFC, and its rank in the enrichment profile (see Materials and Methods for determination of the Avg NFC and rank values). The Avg NFC ranged from 5 to 80. The INFC is also shown. Each mRNA was individually annotated by a database search, and the entire

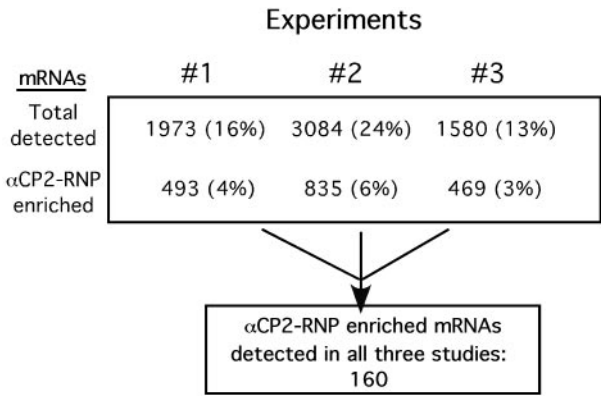

FIG. 2. Summary of three independent microarray analyses of αCP2-associated mRNAs. Three independent studies were carried out to identify mRNAs associated with cytosolic αCP2-RNPs isolated from K562 cells. The total number of mRNAs detected in the αCP2-RNP IPs and the number of mRNAs enriched in each of the αCP2-RNP IPs (relative to the control IP) are shown. The percentages represent the quotient of identified mRNAs to total mRNAs represented on the microarray. The number of mRNAs that were enriched in all three microarray surveys is indicated in the lower box. These consistently detected mRNAs are individually listed in Table 2.

cohort of mRNAs was then organized into a series of subsets according to documented or putative functions. The functional assignments should be considered dynamic because several proteins have multiple functions and could have been assigned to alternative groups. Groups with more than three mRNAs are summarized in Fig. 3. These grouped mRNAs represent 50% of the full list of 160 mRNAs (see Table 2).

The listing of 160 mRNAs represents a nonrandom set of mRNAs. This conclusion is based on the observation that there is no significant correlation between this list and the compilation of unfractionated mRNAs in the cell; of the 160 most abundant mRNAs in total unamplified K562 mRNA, only 7 were present in the αCP2-RNP enriched mRNA population, and of the 160 most abundant mRNAs observed in amplified total K562 RNA, only 6 were present on the list of αCP2-interacting mRNAs. Furthermore, inspection of the sequences of many of the 160 mRNAs revealed several potential αCP binding sites, defined as C- or CU-rich sequences (see above). The presence of α-globin mRNA in the αCP2-RNP mRNA cohort (rank no. 3) supports the validity of the IP-microarray screen. The mRNA with the greatest enrichment (80-fold) in the αCP2-RNP complexes encoded spliceosomal-associated protein 62 kDa (SAP62). Interestingly, another mRNA encoding a spliceosome-associated protein, SAP49, also ranked high on the list, at no. 20. Of note, αCP2 mRNA was present in this list as well; two distinct probe sets on the microarray represent αCP2, and both were enriched in the αCP2-RNP complexes, ranking at nos. 69 and 83. The mRNA encoding mitochondrial thioredoxin (Trx2) ranked at no. 60, and along with 5 other mRNAs, formed a group of mitochondrial enzymes. Of note, we specifically screened the list of 160 αCP2-RNP-associated mRNAs for mRNAs that have been previously proposed as αCP binding targets; only α-globin was found to be in common (see Discussion).

Confirmation of in vivo αCP2-RNP associations by targeted mRNA analysis. Ten mRNAs identified as enriched in the αCP2-RNP complexes by the microarray analysis were chosen for confirmatory studies. Anti-αCP2 or control IP reactions were carried out using fresh K562 extracts, and the copurified mRNAs were directly assayed without prior amplification (Fig. 4). The candidate mRNAs included α-globin, SAP62, SAP49, Trx2, αCP2, c-*src*, junD, a-raf-1, Cln2, and PPT2. Glyceraldehyde-3-phosphate dehydrogenase (GAPDH) and γ-globin mRNAs were assayed in parallel as negative controls. In each assay, the α-globin mRNA demonstrated robust enrichment in the αCP2-RNP population relative to the control IP (Fig. 4A to E, lanes 1 and 2, respectively). Each of the 10 mRNAs identified as enriched in αCP2-RNPs when assayed by microarray hybridization was confirmed to be enriched when independently assayed by targeted RT-PCR analysis of αCP2-RNP preparations. These 10 mRNAs encode SAP49 and Trx2 (Fig. 4A); αCP2, αCP2-KL, and SAP62 (Fig. 4B); the proto-oncoproteins c-*src*, junD, and a-raf-1 (Fig. 4C); and 2 mRNAs which encode factors linked to infantile neuronal ceroid lipofuscinosis, namely, Cln2 and PPT2 (15, 42) (Fig. 4D). CoxII was also tested for interaction with αCP2 by targeted RT-PCR (Fig. 4E). Even though it is not present on the microarray used in these studies, we wanted to assess whether this mRNA interacts with αCP2 because it has been shown previously to be a binding partner of αCP1 (49). Figure 4E shows that coxII mRNA is robustly associated with αCP2-RNPs. eIF3b mRNA was included in one of the studies as an example of an additional sequence on the microarray that was not enriched for in the αCP2-RNPs. Consistent with the microarray screen, the targeted analysis failed to demonstrate enrichment of this mRNA (data not shown). Taken together, the studies confirm the accuracy of the microarray screen for αCP2-associated mRNAs.

The 3′ UTRs of SAP49 and Trx2 mRNAs contain αCP2 binding sites. SAP49 and Trx2 mRNAs were chosen as representatives for further analysis of αCP2 interactions. The specific question was whether the noted in vivo association of these mRNAs with αCP2-RNPs reflected direct binding by αCP2. The focus on 3′ UTR interactions was based on the

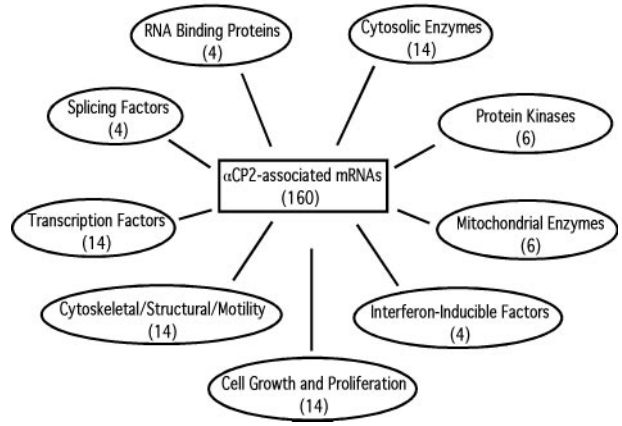

FIG. 3. Major groupings of mRNAs enriched in the αCP2-RNP complexes. The number in parentheses below each category represents the number of mRNAs identified in the group. Note that αCP2 and NFκB are both represented twice on the microarray (see Table 2) but are counted only once in the grouping shown here.

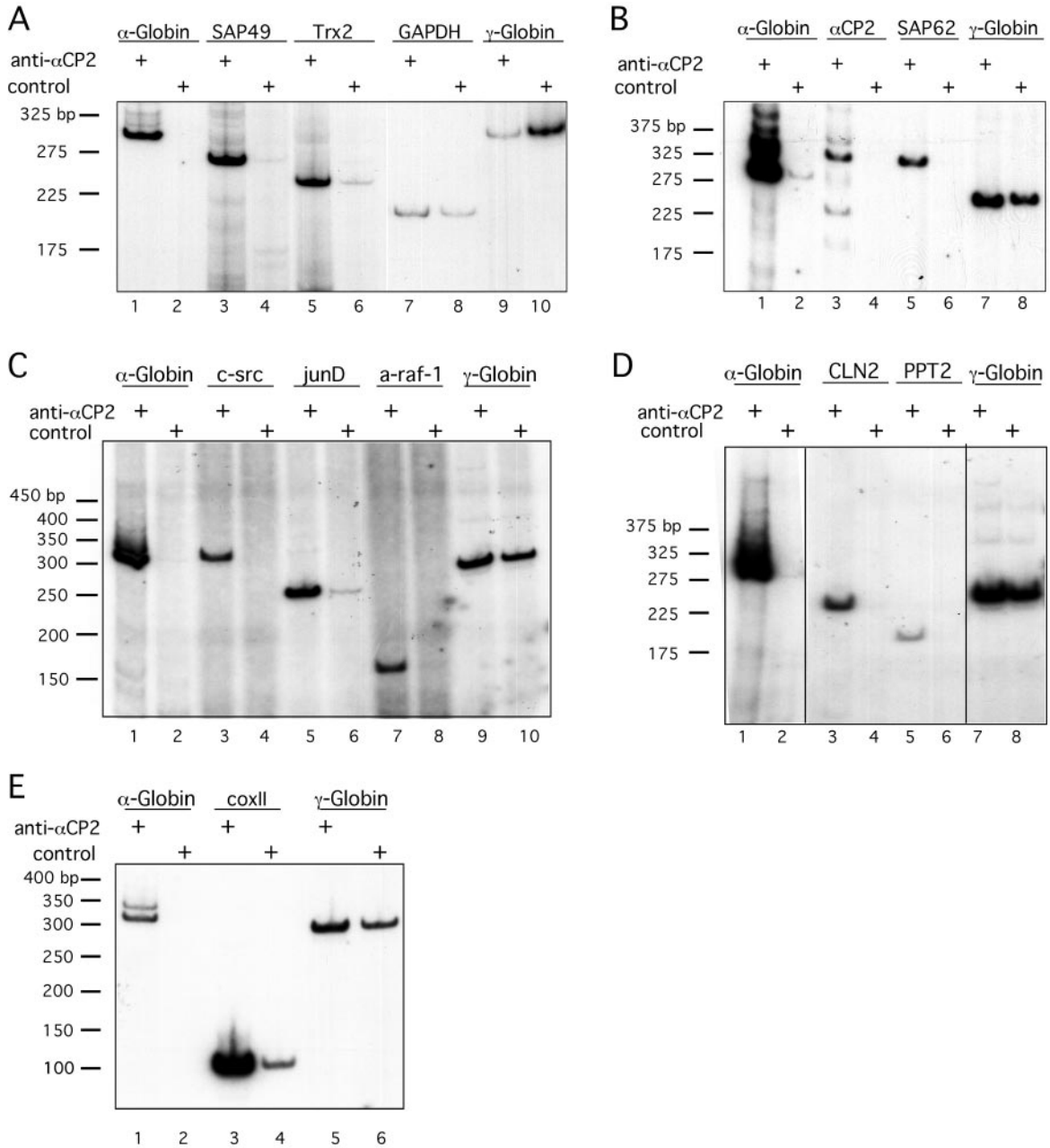

FIG. 4. Confirmation of microarray detection of mRNA enrichment in αCP2-RNP complexes by targeted analysis. Each of the mRNAs noted above the lanes was semiquantitatively assessed by RT-PCR of RNPs isolated with anti-αCP2 or control antisera. In each of the four studies, analysis of α-globin mRNA and γ-globin mRNAs were included as positive and negative controls, respectively. Numbers on the left represent the migration of marker DNA fragments. (A) Analysis of SAP49, Trx2, and GAPDH mRNAs. In this study, GAPDH was included as an additional negative control. (B) Analysis of αCP2 and SAP62 mRNAs. The amplification of the αCP2 mRNA reveals two major bands representing mRNAs encoding αCP2 and αCP2-KL. (C) Analysis of three proto-oncoprotein-encoding mRNAs, c-*src*, junD, and a-raf-1. (D) Analysis of two mRNAs associated with infantile neuronal ceroid lipofuscinosis, Cln2 and PPT2. (E) Analysis of coxII mRNA.

precedent of documented functional interactions between αCPs and 3′ UTRs of other cellular mRNAs (see above). In cases where αCP binding sites have been defined, they contain short patches of C- or CU-rich sequences (2, 12, 35, 36, 38, 45, 52, 53) that are sometimes repeated multiple times (35). Examination of the 3′ UTR of SAP49 reveals 12 potential αCP binding sites defined as a stretch of C's or U's of more than five nucleotides. The Trx2 3′ UTR also contains several CU-rich regions, including four CCCUUCC and three CCUCC repeats that are potential αCP binding sites. The ability of the 3′ UTRs of SAP49 and Trx2 to bind cytoplasmic proteins derived from K562 cells was tested in vitro by EMSA. The 3′ UTR of α-globin mRNA and an actin β-antisense transcript were included as positive and negative controls, respectively (Fig. 5A). The 3′ UTR of SAP49 formed three complexes (designated A, B, and C) with the K562 extract. The Trx2 and α-globin 3′

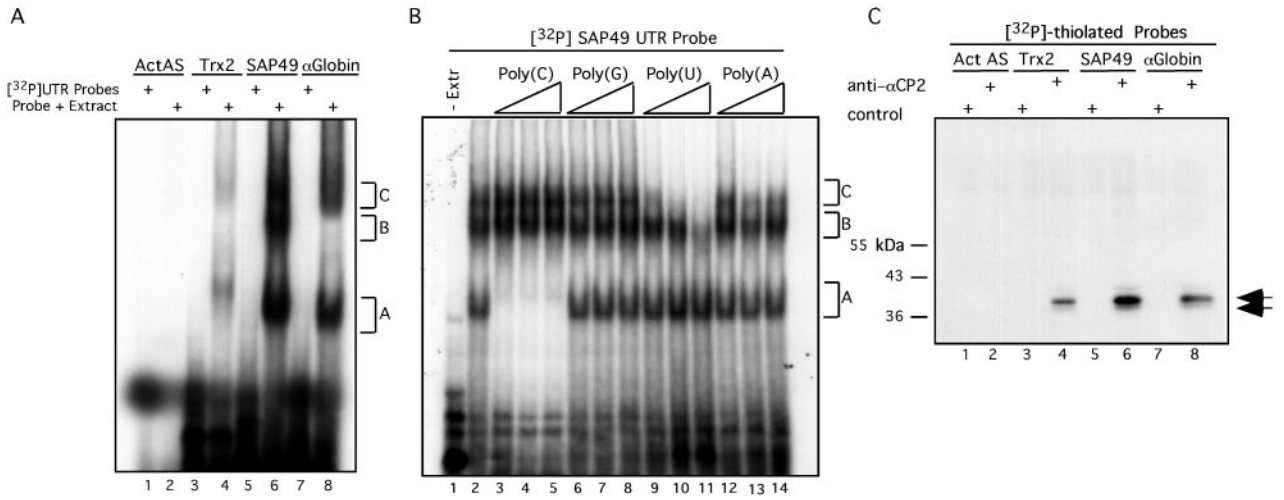

FIG. 5. The 3′ UTRs of SAP49 and Trx2 mRNAs bind directly and specifically to αCP2. (A) RNA EMSA analysis. ^{32}P-labeled RNAs corresponding to the four RNAs indicated at the top of the figure were incubated with K562 extract (Probe + Extract) or without K562 extract ([^{32}P]UTR Probes) as indicated. Three observed RNP complexes are referred to as A, B, or C. β-Actin antisense (ActAS) and α-globin RNAs served as negative and positive controls, respectively. (B) EMSA analysis of the SAP49 3′ UTR in the presence of unlabeled homoribopolymer competitors. Triangles represent increasing amounts of competitor RNA used in the EMSA (10-, 100-, and 500-fold molar excess over the labeled probe). The competitor utilized is indicated above the triangles. (C) UV cross-linking of cytoplasmic proteins to RNA sequences. The same four RNA sequences analyzed by EMSA in Fig. 5A were UV cross-linked to K562 extract and immunoprecipitated with anti-αCP2 or control sera. Numbers on the left represent the migration of marker proteins. The arrows to the right of the autoradiograph indicate the cross-linked products representing αCP2 and αCP2-KL.

UTRs each formed two complexes (designated A and C) with the K562 extract. Complexes A and C were of similar sizes for the three probes (compare lanes 4, 6, and 8) and were specifically absent in the actin antisense RNA incubation (lane 2). Homoribopolymer competition was performed to further test for the presence of αCP in the SAP49 3′ UTR complexes (Fig. 5B). Unlabeled poly(C) competed efficiently and selectively for the fastest complex (complex A) (compare lane 2 with lanes 3 to 5), completely competing even at the lowest concentration of poly(C) tested (10-fold molar excess over the UTR probe [lane 3]). Of note, the migration position of complex A is identical to the previously characterized α-complex formed between αCP and α-globin mRNA (6). In contrast, the other three homoribopolymers had less pronounced effects (lanes 6 to 14). The selective and marked sensitivity of complex A to poly(C) supports the conclusion that the SAP49 3′ UTR can directly bind αCP (for further evidence, see below).

The 3′ UTRs of SAP49 and Trx2 are directly bound by αCP2. UV cross-linking studies were carried out to substantiate a direct interaction of αCP2 with the 3′ UTRs of αCP2-RNP-enriched mRNAs. Radiolabeled and thiolated 3′ UTRs corresponding to the SAP49 or Trx2 3′ UTRs were UV cross-linked to K562 extract. The 3′ UTR of α-globin mRNA and a β-actin antisense transcript were labeled and analyzed in parallel as positive and negative controls, respectively. When the cross-linked products were analyzed by SDS-PAGE, four prominently labeled bands were generated (data not shown). These products appeared to represent nonspecific interactions based on the uniform patterns with the four transcripts and their sensitivity to competition by 18S rRNA. To visualize less abundant complexes that might represent αCP2 binding, the cross-linked products were immunoprecipitated with anti-αCP2 or control antisera (Fig. 5C). Two immunoprecipitated cross-linked products were observed with anti-αCP2 antisera, a 38-kDa band and a less intense 36-kDa band that is seen more clearly on longer exposures (data not shown). These two products (double arrow to the right of the gel) correspond to the sizes of the two major αCP2 isoforms, αCP2 and αCP2-KL. These complexes were detected only when the α-globin, SAP49, and Trx2 3′ UTRs were used as probes in the cross-linking (lanes 4, 6, and 8); no immunoprecipitated cross-linked products were observed using the β-actin antisense RNA (lanes 1 and 2). A series of cross-competition experiments using the 3′ UTRs of Trx2 or SAP49 and human 18S rRNA confirmed that αCP2 specifically interacted with the Trx2 and SAP49 3′ UTRs (data not shown). These studies support the conclusion that αCP2 can directly and specifically bind to the 3′ UTRs of SAP49 and Trx2 mRNAs.

DISCUSSION

We have carried out a microarray analysis of human mRNAs present in a specific subset of cytosolic RNP complexes. These complexes are defined by the presence of αCP2 and αCP2-KL proteins (referred to collectively as αCP2) encoded at the *PCBP*-2 locus. Three independent analyses of the αCP2-RNPs reveal a consistent cohort of 160 mRNAs (Table 2). With the exception of α-globin mRNA, these mRNAs represent novel targets of αCP2 interaction. How αCP2-containing complexes factor into posttranscriptional controls and to what extent such controls might coordinate the expression of subgroups of these mRNAs are questions now open to study.

Several technical aspects and limitations of this approach need to be emphasized. First, the isolation of the αCP2-RNPs depends on IP. It is possible that additional αCP2-RNP complexes are present in the cell but are not recognized in this

procedure due to constraints on protein accessibility and/or subsequent precipitation. Thus, the set of mRNAs identified in this study, while extensive, may not encompass all αCP2-mRNPs. Second, the U95A microarray used in this study contains 12,600 probe sets representing approximately 10,500 unique mRNAs. As current estimates of the number of structural genes in the human genome is in the range of 25,000 or more (28), it is possible that additional targets might be found on subsequent studies using more extensive arrays. Third, the present analysis was limited to cytosolic complexes. The possibility that αCP2 binds to additional transcripts in the nucleus is not presently addressed. Fourth, mRNA sequences from the immunoprecipitated RNPs were amplified in order to generate sufficient probe to interrogate a full microarray. While such a step might alter the representation or abundance of sequences in the population, the validity of utilizing amplified RNA probes is supported by prior reports (40) and was confirmed by a series of control experiments (Fig. 1). Finally, only mRNAs that were enriched (twofold or more) in all three studies were included in the compilation (Table 2). This represents a conservative cutoff. Thus, the 160 mRNAs identified in this report should be considered a reliable but not comprehensive representation of K562 mRNAs present in αCP2-RNP complexes.

It is recognized that the protein contents of the αCP2-RNP complexes are unlikely to be homogeneous in composition. Instead, some of these complexes may contain full-length αCP2, while others may contain the alternative-splice isoform, αCP2-KL. These differences in αCP isoform content may mediate distinct sets of protein-protein interactions, generating diverse macromolecular complexes with distinct functions. αCP2 may also be subject to posttranslational modifications that may regulate the function and/or composition of the complexes (24). Finally, the particular mRNA content of the complexes may dictate the protein composition of the RNP complex via allosteric effects on the binding protein, as has been established for certain protein-DNA interactions (42, 47).

Individual mRNAs identified in the αCP2-RNP complexes may be directly bound by αCP2, or alternatively, their association with αCP2 may be indirect. In the case of human α-globin mRNA, αCP is known to bind directly and uniquely to the C-rich motifs within the 3′ UTR (19). However, it is possible that mRNAs identified in the present survey may be bound by distinct subsets of proteins that are coprecipitated with αCP2 as part of macromolecular αCP2-RNP complexes (22). In the limited sampling of the novel mRNAs associated with the αCP2-RNPs, direct interaction of the mRNA with αCP2 does, in fact, appear to be occurring (Fig. 5). Thus, for at least two of the novel αCP2 mRNPs identified in this study, the specific mRNA inclusion (Trx2 and SAP49) in the complex appears to reflect direct binding by αCP2 as determined for α-globin mRNA.

It is significant that α-globin mRNA was identified in the present screen of αCP2-RNPs and that it constituted the third-most enriched mRNA (Table 2). In contrast, γ-globin mRNA, which is as abundant as α-globin mRNA in K562 cells, was not present in the enriched pool of mRNAs. This selective detection of α-globin mRNA supports the validity of the approach and confirms the association of α-globin mRNA with these complexes in the cell.

Prior to this study, 14 cellular mRNAs had been reported as targets for αCP interaction (see above). Only two of these mRNAs, α-globin and coxII, were identified in the present study. There are multiple reasons for the absence of the remaining mRNAs. mRNAs encoding αI(I) collagen, tyrosine hydroxylase, androgen receptor, 15-lipoxygenase mRNA, PP 2A α, folate receptor α, and erythropoietin are represented on the microarray but were not detected by analysis of total K562 mRNA and thus are probably not present in these cells. Likewise, c/EBPα mRNA, which is not represented on the microarray, could not be detected by targeted RT-PCR of total K562 mRNA (data not shown), consistent with a previous study which showed that this mRNA is not present in K562 cells (41). In contrast, TAPA-1 mRNA (see above) is detected in microarray analysis of total K562 RNA but is not enriched in the immunopurified αCP2-RNPs. This may reflect the fact that TAPA-1 was identified as a target of αCP1 by prior studies and may be specific to this isoform (49).

Coordination of posttranscriptional controls by particular RNA-binding proteins may occur at a number of steps. We have previously suggested that the α-complex may constitute a common determinant of high-level stability (18). The identification in the present survey of 160 mRNA targets of αCP2 can now be used to further test this premise. Fourteen of these mRNAs encode structural cytoskeletal components or proteins involved with cell motility. It is likely that these are long-lived mRNAs based on the premise that proteins that do not need to be acutely controlled are usually encoded by highly stable mRNAs (45). A second well-defined function of αCP is in translation control. Identifying whether any of the 160 cellular mRNAs are subject to this level of control would establish another provisional basis for potential coordination of gene expression by αCP2-RNP complexes.

mRNAs encoding 11 enzymes were present in the αCP2-RNP population. Two of these enzymes are linked to the pathogenesis of the neurodegenerative disorder infantile neuronal ceroid lipofuscinosis (15, 43). The identification of these two enzymes, lysosomal pepstatin-insensitive protease (Cln2) (rank no. 54) and palmitoyl-protein thioesterase 2 (PPT2) (rank no. 103), suggests that αCP2 might act as a modifier of phenotype in this disease by regulating the available levels of these two enzymes in a coordinate manner. It is also of note that 6 of the 20 total enzyme-encoding mRNAs in the αCP2-RNP population direct the synthesis of enzymes specific to the mitochondria. Two of the six mRNAs identified in an independent screen for αCP1-associated mRNAs also encoded mitochondrial localized proteins (49). These data suggest that αCPs may coordinate aspects of mitochondrial function or mRNA localization via posttranscriptional mechanisms.

Thirteen αCP2-associated mRNAs encode transcription factors. The potential involvement of αCP2 in transcription factor expression is consistent with a report showing that αCP2 regulates translation of the mRNA encoding the transcription factor, c/EBPα (39). It is also of interest that JunD mRNA is enriched in the αCP2-RNPs. Expression of JunD is regulated at the posttranscriptional level (27) by alterations in mRNA stability in response to cellular levels of polyamines. The association of αCP2 with JunD mRNA in the present study establishes a testable model in which αCP2 may play a role in this process. Thus, both translation and stability controls may be in play via αCP2 association with transcription factor mRNAs.

The presence of four mRNAs encoding interferon-inducible factors in the αCP2 RNPs is intriguing, as five different viruses have been reported to utilize αCP to regulate viral gene expression (see above). Since interferon is an antiviral agent, it is possible that these viruses have evolved structures that allow them to sequester αCP2 from these cellular mRNAs. For example, if αCP2 enhances the expression of specific interferon-inducible genes, sequestration of αCP2 by viral RNAs would inhibit the antiviral response while at the same time possibly enhancing their own expression (3, 4, 11, 12, 33, 51). The demonstration that expression of RNA decoys can block the functional interaction of αCPs with target RNAs in vivo supports several assumptions underlying this model (30).

A final note concerns αCP2 mRNA. The enrichment of αCP2 mRNA in αCP2-RNP complexes was confirmed by two separate probe sets on the microarray (Table 2) and substantiated by directed RT-PCR analysis (Fig. 4B). This association suggests that αCP2 expression may be subject to posttranscriptional autoregulation. A negative autoregulatory loop might mediate tight control over synthesis of the final αCP2 product, while a positive loop might amplify the expression of αCP2 in certain situations. Further mapping of this interaction and the corresponding mechanistic pathway(s) involved in the proposed autoregulation of αCP2 expression are of interest for further study.

ACKNOWLEDGMENTS

This work was supported by NIH grants RO1 HL 65449 and PO1-CA72765 to S.A.L. The support of the Doris Duke Foundation is gratefully acknowledged. S.A.W is a recipient of an NRSA fellowship 5 F32 GM063396-02 from the National Institutes of Health.

We thank Gregg Johannes for critical reading of the manuscript and experimental advice.

REFERENCES

1. **Aasheim, H. C., T. Loukianova, A. Deggerdal, and E. B. Smeland.** 1994. Tissue specific expression and cDNA structure of a human transcript encoding a nucleic acid binding [oligo(dC)] protein related to the pre-mRNA binding protein K. Nucleic Acids Res. **22:**959–964.
2. **Andino, R., G. Rieckhof, P. L. Achacose, and D. Baltimore.** 1993. Poliovirus RNA synthesis utilizes an RNP complex formed around the 5′ end of viral RNA. EMBO J. **12:**3587–3598.
3. **Blyn, L. B., K. M. Swiderek, O. Richards, D. C. Stahl, B. L. Semler, and E. Ehrenfeld.** 1996. Poly(rC) binding protein 2 binds to stem-loop IV of the poliovirus RNA 5′ noncoding region: identification by automated liquid chromatography-tandem mass spectrometry. Proc. Natl. Acad. Sci. USA **93:**11115–11120.
4. **Blyn, L. B., J. S. Towner, B. L. Semler, and E. Ehrenfeld.** 1997. Requirement of poly(rC) binding protein 2 for translation of poliovirus RNA. J. Virol. **8:**6243–6246.
5. **Brown, V., P. Jin, S. Ceman, J. C. Darnell, W. T. O'Donnell, S. A. Tenenbaum, X. Jin, Y. Feng, K. D. Wilkinson, J. D. Keene, R. B. Darnell, and S. T. Warren.** 2001. Microarray identification of FMRP-associated brain mRNAs and altered mRNA translational profiles in fragile X syndrome. Cell **107:** 477–487.
6. **Chkheidze, A. N., D. L. Lyakhov, A. V. Makeyev, J. Morales, J. Kong, and S. A. Liebhaber.** 1999. Assembly of the α-globin mRNA stability complex reflects binary interaction between the pyrimidine-rich 3′ untranslated region determinant and poly(C) binding protein αCP. Mol. Cell. Biol. **19:**4572–4581.
7. **Collier, B., L. Goobar-Larsson, M. Sokolowski, and S. Schwartz.** 1998. Translational inhibition in vitro of human papillomavirus type 16 L2 mRNA mediated through interaction with heterogenous ribonucleoprotein K and poly(rC)-binding proteins 1 and 2. J. Biol. Chem. **273:**22648–22656.
8. **Crichton, R. R., S. Wilmet, R. Legssyer, and R. J. Ward.** 2002. Molecular and cellular mechanisms of iron homeostasis and toxicity in mammalian cells. J. Inorg. Biochem. **91:**9–18.
9. **Czyzyk-Krzeska, M. F., and A. C. Bendixen.** 1999. Identification of the poly(C) binding protein in the complex associated with the 3′ untranslated region of erythropoietin messenger RNA. Blood **6:**2111–2120.
10. **Funke, B., R. Zuleger, R. Benavente, T. Schuster, M. Goller, J. Stevenin, and I. Horak.** 1996. The mouse poly(C)-binding protein exists in multiple isoforms and interacts with several RNA-binding proteins. Nucleic Acids Res. **24:**3821–3828.
11. **Gamarnik, A. V., and R. Andino.** 1997. Two functional complexes formed by KH domain containing proteins with the 5′ noncoding region of poliovirus RNA. RNA **3:**882–892.
12. **Gamarnik, A. V., and R. Andino.** 2000. Interactions of viral protein 3CD and poly(rC) binding protein with the 5′ untranslated region of the poliovirus genome. J. Virol. **74:**2219–2226.
13. **Gibson, T. J., J. T. Thompson, and J. Heringa.** 1993. The KH domain occurs in a diverse set of RNA-binding proteins that include the antiterminator NusA and is probably involved in binding to nucleic acid. FEBS Lett. **324:** 361–366.
14. **Graff, J., J. Cha, L. B. Blyn, and E. Ehrenfeld.** 1998. Interaction of poly(rC) binding protein 2 with the 5′ noncoding region of hepatitis A virus RNA and its effects on translation. J. Virol. 1998. **72:**9668–9675.
15. **Gupta, P., A. A. Soyombo, A. Atashband, K. E. Wisniewski, J. M. Shelton, J. A. Richardson, R. E. Hammer, and S. L. Hofmann.** 2001. Disruption of PPT1 or PPT2 causes neuronal ceroid lipofuscinosis in knockout mice. Proc. Natl. Acad. Sci. USA **98:**13566–13571.
16. **Gutierrez-Escolano, A. L., Z. U. Brito, R. M. delAngel, and X. Jiang.** 2000. Interaction of cellular proteins with the 5′ end of Norwalk virus genomic RNA. J. Virol. **74:**8558–8562.
17. **Hieronymus, H., and P. A. Silver.** 2003. Genome-wide analysis of RNA-protein interactions illustrates specificity of the mRNA export machinery. Nat. Genet. **33:**155–161.
18. **Holcik, M., and S. A. Liebhaber.** 1997. Four highly stable eukaryotic mRNAs assemble 3′ untranslated region RNA-protein complexes sharing cis and trans components. Proc. Natl. Acad. Sci. USA **94:**2410–2414.
19. **Ji, X., J. Kong, and S. A. Liebhaber.** 2003. In vivo association of the stability control protein αCP with actively translating mRNAs. Mol. Cell. Biol. **23:** 899–907.
20. **Johannes, G., and P. Sarnow.** 1998. Cap-independent polysomal association of natural mRNAs encoding c-myc, BiP, and eIF4G conferred by internal ribosome entry sites. RNA **4:**1500–1513.
21. **Keene, J. D., and S. A. Tenenbaum.** 2002. Eukaryotic mRNPs may represent posttranscriptional operons. Mol. Cell **9:**1161–1167.
22. **Kiledjian, M., C. T. DeMaria, G. Brewer, and K. Novick.** 1997. Identification of AUF1 (heterogeneous nuclear ribonucleoprotein D) as a component of the α-globin mRNA stability complex. Mol. Cell. Biol. **17:**4870–4876.
23. **Kiledjian, M., X. Wang, and S. A. Liebhaber.** 1995. Identification of two KH domain proteins in the α-globin mRNP stability complex. EMBO J. **14:**4357–4364.
24. **Leffers, H., K. Dejgaard, and J. E. Celis.** 1995. Characterization of two major cellular poly(rC)-binding human proteins, each containing three K-homologous (KH) domains. Eur. J. Biochem. **230:**447–453.
25. **Lewis, H. A., H. Chen, C. Edo, R. J. Buckanovich, Y. Y. L. Yang, K. Musunuru, R. Zhong, R. B. Darnell, and S. K. Burley.** 1999. Crystal structures of Nova-1 and Nova-2-homology RNA-binding domains. Structure **7:**191–203.
26. **Lewis, H. A., K. Musunuru, K. B. Jensen, C. Edo, H. Chen, R. B. Darnell, and S. K. Burley.** 2000. Sequence-specific RNA binding by a Nova KH-domain: implications for paraneoplastic disease and the fragile X syndrome. Cell **100:**323–332.
27. **Li, L., L. Liu, J. N. Rao, A. Esmaili, E. D. Strauch, B. L. Bass, and J. Y. Wang.** 2002. JunD stabilization results in inhibition of normal intestinal epithelial cell growth through P21 after polyamine depletion. Gastroenterology **123:**764–769.
28. **Makalowski, W.** 2001. The human genome structure and organization. Acta Biochim. Pol. **48:**587–598.
29. **Makeyev, A. V., A. N. Chkheidze, and S. A. Liebhaber.** 1999. A set of highly conserved RNA-binding proteins, alphaCP-1 and alphaCP-2, implicated in mRNA stabilization, are coexpressed from an intronless gene and its intron-containing paralog. J. Biol. Chem. **35:**24849–24857.
30. **Makeyev, A. V., D. Eastmond, and S. A. Liebhaber.** 2002. Targeting a KH-domain protein with RNA decoys. RNA **8:**1160–1173.
31. **Makeyev, A. V., and S. A. Liebhaber.** 2000. Identification of two novel mammalian genes establishes a subfamily of KH-domain RNA-binding proteins. Genomics **67:**301–316.
32. **Makeyev, A. V., and S. A. Liebhaber.** 2002. The poly(C)-binding proteins: a multiplicity of functions and a search for mechanisms. RNA **8:**265–278.
33. **Murray, K. E., A. W. Roberts, and D. J. Barton.** 2001. Poly(rC) binding proteins mediate poliovirus mRNA stability. RNA **7:**1126–1141.
34. **Ostareck-Lederer, A., D. H. Ostareck, and M. W. Hentze.** 1998. Cytoplasmic regulatory functions of the KH-domain proteins hnRNPs K and E1/E2. Trends Biochem. Sci. **23:**409–411.
35. **Ostareck, D. H., A. Ostareck-Lederer, M. Wilm, B. J. Thiele, M. Mann, and M. W. Hentze.** 1997. mRNA silencing in erythroid differentiation: hnRNP K and hnRNP E1 regulate 15-Lipoxygenase translation from the 3′ end. Cell **89:**597–606.
36. **Paillard, L., D. Maniey, P. Lachaume, V. H. Legagneux, and B. Osborne.**

2000. Identification of a C-rich element as a novel cytoplasmic polyadenylation element in Xenopus embryos. Mech. Dev. **93:**117–125.
37. **Parsley, T. B., J. S. Towner, L. B. Blyn, E. Ehrenfeld, and B. L. Semler.** 1997. Poly (rC) binding protein 2 forms a ternary complex with the 5′-terminal sequences of poliovirus RNA and the viral 3CD proteinase. RNA **3:**1124–1134.
38. **Paulding, W. R., and M. F. Czyzyk-Krzeska.** 1999. Regulation of tyrosine hydroxylase mRNA stability by protein-binding, pyrimidine-rich sequence in the 3′-untranslated region. J. Biol. Chem. **274:**2532–2538.
39. **Perrotti, D., V. Cesi, R. Trotta, C. Guerzoni, G. Santilli, K. Campbell, A. Iervolino, F. Condorelli, C. Gambacorti-Passerini, M. A. Caligiuri, and B. Calabretta.** 2002. BCR-ABL suppresses C/EBPalpha expression through inhibitory action of hnRNP E2. Nat. Genet. **30:**48–58.
40. **Phillips, J., and J. H. Eberwine.** 1996. Antisense RNA amplification: a linear amplification method for analyzing the mRNA population from single living cells. Methods **10:**283–288.
41. **Radomska, H. S., C. S. Huettner, P. Zhang, T. Cheng, D. T. Scadden, and D. G. Tenen.** 1998. CCAAT/enhancer binding protein α is a regulatory switch sufficient for induction of granulocytic development from bipotential myeloid progenitors. Mol. Cell. Biol. **18:**4301–4314.
42. **Scully, K. M., E. M. Jacobson, K. Jepsen, V. Lunyak, H. Viadiu, C. Carriere, D. W. Rose, F. Hooshmand, A. K. Aggarwal, and M. G. Rosenfeld.** 2000. Allosteric effects of Pit-1 DNA sites on long-term repression in cell type specification. Science **290:**1127–1131.
43. **Sleat, D. E., R. J. Donnelly, H. Lackland, C. G. Liu, I. Sohar, R. K. Pullarkat, and P. Lobel.** 1997. Association of mutations in a lysosomal protein with classical late-infantile neuronal ceroid lipofuscinosis. Science **277:**1802–1805.
44. **Spangberg, K., and S. Schwartz.** 1999. Poly(C)-binding protein interacts with the hepatitis C virus 5′ untranslated region. J. Gen. Virol. **80:**1371–1376.
45. **Stefanovic, B., C. Hellerbrand, M. Holcik, M. Briendl, S. A. Liebhaber, and D. A. Brenner.** 1997. Posttranscriptional regulation of collagen α1(I) mRNA in hepatic stellate cells. Mol. Cell. Biol. **17:**5201–5209.
46. **Tenenbaum, S. A., P. J. Lager, C. C. Carson, and J. D. Keene.** 2002. Ribonomics: identifying mRNA subsets in mRNP complexes using antibodies to RNA-binding proteins and genomic arrays. Methods **26:**191–198.
47. **Tomilin, A., A. Remenyi, K. Lins, H. Bak, S. Leidel, G. Vriend, M. Wilmanns, and H. R. Scholer.** 2000. Synergism with the coactivator OBF-1 (OCA-B, BOB-1) is mediated by a specific POU dimer configuration. Cell **103:**853–864.
48. **Tommerup, N., and H. Leffers.** 1996. Assignment of human KH-box-containing genes by in situ hybridization: HNRNPK maps to 9q21.32-q21.33, PCBP1 to 2p12-p13, and PCBP2 to 12q13.12-q13.13, distal to FRA12A. Genomics **32:**297–298.
49. **Trifillis, P., N. Day, and M. Kiledjian.** 1999. Finding the right RNA: identification of cellular mRNA substrates for RNA-binding proteins. RNA **5:**1071–1082.
50. **Waggoner, S., and P. Sarnow.** 1998. Viral ribonucleoprotein complex formation and nucleolar-cytoplasmic relocalization of nucleolin in poliovirus-infected cells. J. Virol. **72:**6699–6709.
51. **Walter, B. L., J. H. C. Nguyen, E. Ehrenfeld, and B. Semler.** 1999. Differential utilization of poly(rC) binding protein 2 in translation directed by picornavirus IRES elements. RNA **5:**1570–1585.
52. **Wang, X., M. Kiledjian, I. M. Weiss, and S. A. Liebhaber.** 1995. Detection and characterization of a 3′ untranslated region ribonucleoprotein complex associated with human α-globin mRNA stability. Mol. Cell. Biol. **15:**1769–1777.
53. **Weiss, I. M., and S. A. Liebhaber.** 1995. Erythroid cell-specific mRNA stability elements in the α2-globin 3′ nontranslated region. Mol. Cell. Biol. **15:**2457–2465.
54. **Xiao, X., Y. S. Tang, J. Y. Mackins, X. L. Sun, H. N. Jayaram, D. K. Hansen, and A. C. Antony.** 2001. Isolation and characterization of a folate receptor mRNA-binding trans-factor from human placenta. Evidence favoring identity with heterogeneous nuclear ribonucleoprotein E1. J. Biol. Chem. **276:**41510–41517.
55. **Yeap, B. B., D. C. Voon, J. P. Vivian, R. K. McCulloch, A. M. Thomson, K. M. Giles, M. F. Czyzyk-Krzeska, H. Fuurneaux, M. C. J. Wilce, J. A. Wilce, and P. J. Leedman.** 2002. Novel binding of HuR and poly(C)-binding protein to a conserved UC-rich motif within the 3′-untranslated region of the androgen receptor messenger RNA. J. Biol. Chem. **277:**27183–27192.